Electronic phase transition between localized and itinerant states in the solid-solution system $CaCu_3Ti_{4-x}Ru_xO_{12}$

Ting-Hui Kao,[1,2] Hiroya Sakurai,[1,*] Shan Yu,[1] Harukazu Kato,[3] Naohito Tsujii,[1] and Hung-Duen Yang[2]

[1]*National Institute for Materials Science, 1-1 Namiki, Tsukuba 305-0044, Japan*

[2]*Department of Physics, National Sun Yat-Sen University, Kaohsiung 804, Taiwan*

[3]*Faculty of Science, Kochi University, 2-5-1 Akebono-cho, Kochi 780-8520, Japan*

(Received 11 November 2016; revised manuscript received 27 February 2017; published 18 May 2017)

A solid solution between $CaCu_3Ti_{4-x}Ru_xO_{12}$ end members was first synthesized using a high-pressure technique. The residual magnetization at 2 K sharply changes at $2 \leqslant x \leqslant 3$, and a spin-glass-like phase suddenly disappears at $x = 2.5$, suggesting a first-order electronic phase transition. The magnetic susceptibility shows a strong dependence on the temperature for $x \leqslant 1$ and a weak dependence for $x \geqslant 3$. At an intermediate value of x, the weak dependence at high temperatures changes to a strong dependence at low temperatures. The electrical resistivity shows variable-range-hopping-type behavior for $x \leqslant 1$ and metallic behavior for $x \geqslant 3.5$, changing from the latter to the former at $T_\rho \sim 150$, 8.5, and 3.5 K for $x = 2.0$, 2.5, and 3.0, respectively. An electronic phase diagram based on these results is similar to that for an organic system showing a Mott transition and to a theoretical diagram for the Mott transition. Considering electronic band structure calculations, the local magnetic moments at the CuO_4 squares of the Ti compound become itinerant with increasing Ru content by means of a first-order phase transition, suggesting that the transition can be regarded as a Mott transition. The Mott transition is unique in that the atomic orbitals of the Ru cations play an important role in the increased hopping amplitude of the electrons/holes of the CuO_4 molecularlike orbitals.

DOI: 10.1103/PhysRevB.95.195141

I. INTRODUCTION

Transition-metal oxides show a variety of electronic properties because of their d or f electrons. Their properties are usually understood using two major approaches: localized- and itinerant-electron models. In the localized-electron model, the electrons are located only at the transition-metal ions, having spin angular momenta or total angular momenta. In the itinerant-electron model, electrons move in the electronic bands, which extend over the entire crystal. Most of the spin degree of freedom in this case disappears owing to the Fermi degeneracy. Thus, the magnetic properties are attributed only to the electrons/holes near the Fermi level. In contrast, the intermediate electronic states between the two models remain unclear, although interesting properties such as unconventional superconductivity occur there. In particular, it is not well understood how local magnetic moments vanish and emerge in the intermediate states. For example, there is no clear picture of metallic antiferromagnets; some antiferromagnets show Curie-Weiss behavior with large Curie constants, although they have Fermi surfaces. The Fermi degeneracy appears to not apply to them, and the origin of the large Curie constants is still unclear.

The crossover between localized- and itinerant-electron states may occur via a phase transition. For example, the Mott transition [1] and valence transition [2,3] are well-known phase transitions. Although these transitions are usually first order, a second-order phase transition has also been proposed; according to Doniach phase diagram, the antiferromagnetically ordered state with Ruderman-Kittel-Kasuya-Yosida interactions changes into a Kondo state passing a quantum critical point [4]. In contrast, a crossover without a transition has been observed in heavy-fermion systems, in which local magnetic moments emerge by thermal excitation from Kondo singlet states. Of course a crossover without a transition also occurs near the Mott transition or valence transitions at high temperatures above the critical end points of the first-order phase transition lines [1–3]. In this paper we show which type of change takes place in the solid-solution system of $CaCu_3Ti_{4-x}Ru_xO_{12}$.

$CaCu_3Ti_4O_{12}$ and $CaCu_3Ru_4O_{12}$ are isostructural with one another, having A-site ordered perovskite structures. As Fig. 1 illustrates, Ca and Cu ions occupy the A sites in the perovskite structure with atomic order, while the Ti and Ru ions occupy the B sites. The Cu site is coordinated by four close oxygen atoms among the 12 oxygen atoms originally coordinated around the A site in conventional perovskites, forming CuO_4 squares. There are three types of CuO_4 squares distinguished by their normals; a CuO_4 square is parallel to the ab, bc, or ac plane. The Ti compound is electrically insulating with a giant dielectric constant above approximately 100 K [5,6]. The Cu ions have a $3d^9$ electronic configuration; thus they have local magnetic moments with $S = 1/2$. The magnetic moments antiferromagnetically order at $T_N = 27$ K [7]. On the other hand, the Ru compound shows metallic conductivity with a Sommerfeld constant of $\gamma \sim 88$ mJ/(mol K^2) [8,9]. It was originally regarded as a heavy fermion compound because the Sommerfeld constant appeared to be relatively large and because its magnetic susceptibility displays a broad maximum at approximately 200 K, as in the case of $CeSn_3$, a typical Kondo compound [8]. However, recent nuclear magnetic resonance (NMR) experiments have clearly demonstrated the absence of local magnetic moments up to a temperature as high as 700 K, thus ruling out the Kondo-lattice picture [10]. Electronic band structure calculations point out that the band mass of a carrier is not significantly different from the mass expected from the Sommerfeld constant [11]. Furthermore, it has been reported that the Sommerfeld constant

*sakurai.hiroya@nims.go.jp

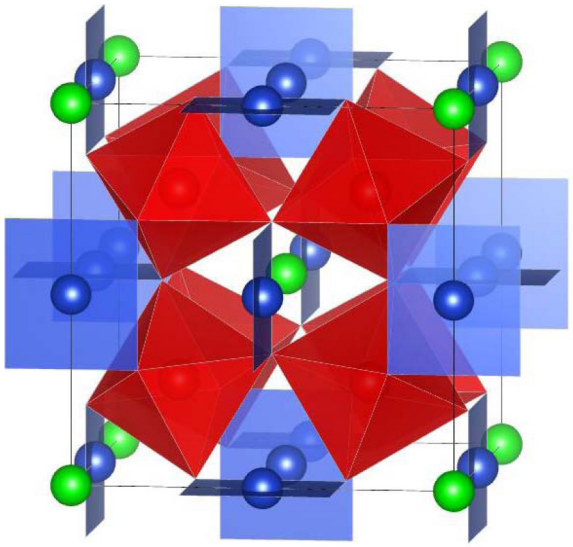

FIG. 1. Crystal structure of $CaCu_3M_4O_{12}$ (M = Ti, Ru). The oxygen sites occupy the corners of the squares and octahedra. The spheres (green), squares (blue), and octahedra (red) are Ca ions, CuO_4 squares, and RuO_6 octahedra, respectively. The lines connecting the Ca sites show the unit cell.

is suppressed rather than enhanced [12,13]. Although these results indicate that the Ru compound is not a typical Kondo compound, the metallic state is obviously unconventional because both the ratios of the specific heat to the temperature and the spin-lattice relaxation rate to the temperature show unusual logarithmic enhancements below 2 K [14]. The origin of this non-Fermi liquid behavior still remains unclear.

Pioneering work on a solid solution of $CaCu_3Ti_{4-x}Ru_xO_{12}$ compounds was reported concurrently with the discovery of the "heavy" mass of the Ru compound [8,9]. The motivation for investigating the solid solution is understandable because evidence of the existence of local magnetic moments at Cu sites was key to supporting the Kondo picture for the Ru compound. However, the solid solution was limited up to $x \simeq 1.5$ [8]. Thus, no clear conclusion about the local magnetic moments in the Ru compound was obtained. In the present study, we first found that an entire solid solution could be achieved using a high-pressure and high-temperature synthesis technique. Using samples with various Ru contents, the magnetic properties, specific heat, and electrical resistivity were measured, leading to the finding that drastic changes in the electronic states occur at $2 \leqslant x \leqslant 3$.

II. EXPERIMENT

Powder samples of $CaCu_3Ti_{4-x}Ru_xO_{12}$ ($0 \leqslant x \leqslant 4$) were fabricated from stoichiometric mixtures of CaO, CuO, TiO_2, and RuO_2. The raw materials were weighed and mixed in a glove box filled with Ar gas because CaO reacts with the water and carbon dioxide in air. CaO was prepared by firing $CaCO_3$ twice in an Ar gas flow at 1000 °C in a tube furnace connected to the glove box. The mixtures for the $x \neq 0$ samples were sealed in Au or Pt capsules in the glove box, pressed at 7.7 GPa by a belt-type press, and heated to 1300−1600°C. After synthesis, the temperature was rapidly reduced to room temperature, and then the pressure was gradually released. $CaCu_3Ti_4O_{12}$ was synthesized in air at 1000 °C without being sealed in a capsule. The sample was pressed into a pellet and fired twice. After the second sintering, the sample was slowly cooled to the ambient temperature in a furnace to reduce the number of crystal defects.

The samples were characterized by powder x-ray diffraction (XRD) measurements with Cu K_α radiation using a x-ray diffractometer (MiniFlex 600, Rigaku Corporation, Tokyo, Japan) equipped with a x-ray detector (D/teX Ultra 2, Rigaku Corporation, Tokyo, Japan). Magnetic data were collected using a magnetic-property measurement system (MPMS, Quantum Design, Inc., San Diego, California, USA). The thermal- and electrical-property measurements were performed using a physical-property measurement system (PPMS, Quantum Design, Inc., San Diego, California, USA). In this paper the temperature, magnetic field, magnetic susceptibility, specific heat, and electrical resistivity are represented by T, H, χ, C_P, and ρ, respectively. The magnetic susceptibility is defined simply as $\chi = M/H$, where M is the magnetization.

III. RESULTS

A. Phase characterization

Figure 2 shows the XRD patterns of the $x = 1.0$ samples fabricated at 1300 and 1500 °C. Figures 2(b) and 2(c) clearly show that the XRD peaks for the former sample are split into

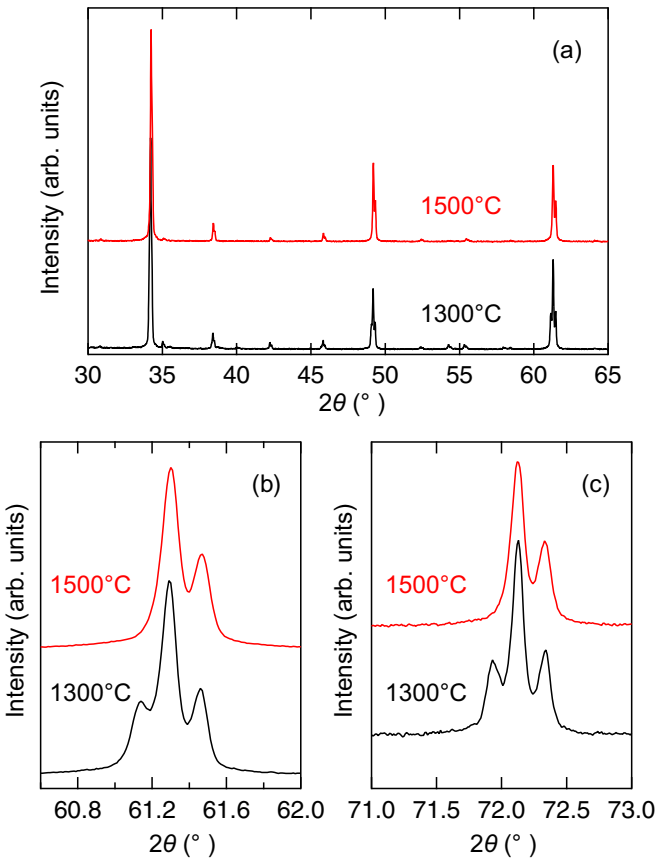

FIG. 2. XRD patterns of $CaCu_3Ti_{3.0}Ru_{1.0}O_{12}$ samples created at 1300 °C (bottom/black) and 1500 °C (top/red). (b) and (c) Different views of the XRD pattern in (a).

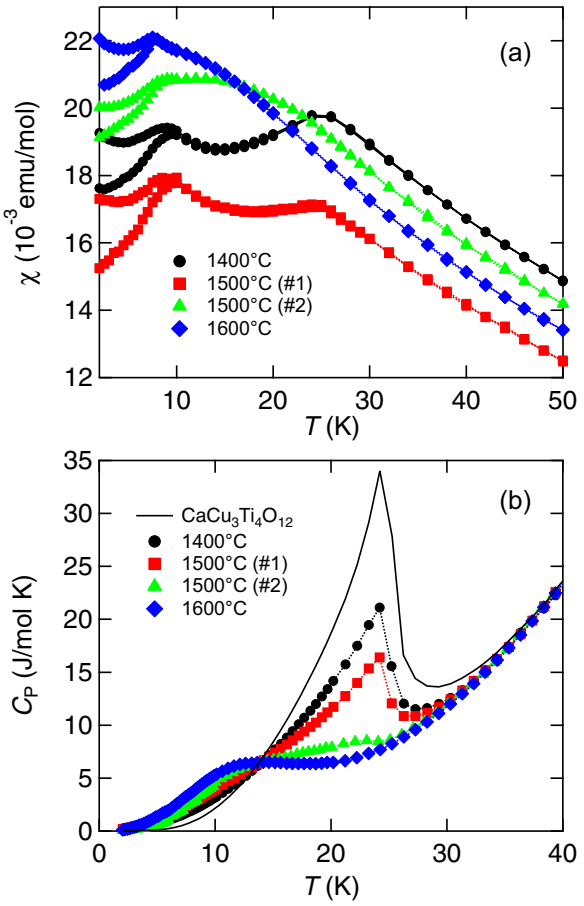

FIG. 3. (a) Magnetic susceptibility and (b) specific heat of $CaCu_3Ti_{3.5}Ru_{0.5}O_{12}$ samples fabricated at various temperatures. The magnetic susceptibility was measured at approximately 10 Oe. The small magnetic field may include a relatively large error, which would make the absolute values of the susceptibility inaccurate. An error of about 1 Oe can explain the differences in the susceptibility among the samples at 50 K.

two sets of $K_{\alpha 1}$ and $K_{\alpha 2}$ peaks. Thus the sample is phase separated into two phases of Ti-rich and Ru-rich phases with different lattice constants, as is sometimes observed in solid-solution systems [15–17]. In contrast, the XRD peaks for the latter sample are composed of a single set, indicating that the sample is chemically homogeneous.

For the $x = 0.5$ sample fabricated at 1400 °C, no clear split in the XRD peaks was detected, although the sample was phase separated, as mentioned below. This is because the nominal composition is close to the Ti-rich phase; the volume fraction of the Ti-rich phase is very large such that the XRD peaks of the minor phase are undetectable. A clear signature of the phase separation is observed from the magnetic susceptibility, as shown in Fig. 3(a). The samples fabricated at 1400 and 1500 °C both exhibited a peak around T_N and spin-glass-like separation between the zero-field-cooling (ZFC) and field-cooling (FC) values below $T_{SG} \simeq 8$ K. This peak arises from the Ti-rich phase because it corresponds to the antiferromagnetic order of the Ti-pure compound. In contrast, the spin-glass-like separation is due to the Ru-rich phase because the spin-glass-like transition appears in the chemically uniform samples for $0.5 \leqslant x \leqslant 2.5$, as will be shown later. The specific heat also shows the phase separation, as shown in Fig. 3(b). The sample fabricated at 1400 °C shows a clear peak around T_N and a larger tail at lower temperatures than the tail of the Ti-pure sample. The larger tail is due to the contribution from the Ru-rich phase, which causes the hump at T_{SG}, as shown later. The peak and large tail are also observed for the samples fabricated at 1500 °C; therefore, they are still phase separated. However, it should be noted that two samples, 1 and 2, fabricated at 1500 °C, have quantitatively different values of the magnetic susceptibility and specific heat; sample 2 shows only small anomalies at T_N. This suggests that the chemical phase separation disappears just above 1500 °C at 7.7 GPa. The quantitative difference is probably due to the inevitable differences in the synthesis conditions, such as the small differences in the pressure and temperature gradients within the small space of the press. Indeed, the sample fabricated at 1600 °C is chemically uniform, showing no peak at T_N in the magnetic susceptibility or specific heat. From these results, the synthesis temperature of 1500 °C is inadequate for fabricating a chemically uniform sample for $x = 0.5$, although it is adequate for $x = 1.0$. In contrast, the samples for $x \geqslant 3$ showed no chemical phase separation, even at 1300 °C. Thus, the phase separation occurs at higher temperatures for smaller values of x. More details about the phase separation are presented in the Supplemental Material [18].

In a previous report [8], no phase separation was suggested for samples with $x \leqslant 1.5$, which were fabricated in air, although they were synthesized at much lower temperatures in the range of 1000−1050 °C. Two possibilities can be considered to account for the discrepancy in the phase separation between the samples fabricated in air and those fabricated at a high pressure. First, either Ru or O defects (or both), introduced when the samples were fired in air [19], may have stabilized the homogeneous solid solution in the small range of x. The magnetic properties of the ambient-pressure sample with a certain Ru content seem to correspond to those of the high-pressure sample with a slightly higher Ru content. This implies that the actual Ru content of the former sample was lower than that of the nominal sample owing to the vaporization of Ru ions [19]. RuO_2 is volatilized above 900° in air [15]. Second, the high pressure may change x and the temperature ranges of the phase separation.

The lattice constants of the samples without the chemical phase separation are shown in Fig. 4. These constants slightly increase with increasing x, indicating that the solid solution has successfully formed. The small change is caused by the similar ionic radii of the Ti and Ru ions. Hereafter, only the results obtained using the samples without the chemical phase separation will be shown. It should be emphasized that the chemical phase separation is caused by atomic segregation. Thus, it differs from electronic phase separation, which can occur even in a uniform matrix. Indeed, theoretical calculations, without assuming chemical inhomogeneity, predict the electronic phase separations for some systems such as high-T_C cuprates [20,21].

B. Magnetic properties

Figures 5(a) and 5(b) show the reciprocal magnetic susceptibility measured at 1 T. The values of the susceptibility of the Ti- and Ru-pure samples agree well with previous results [8,9].

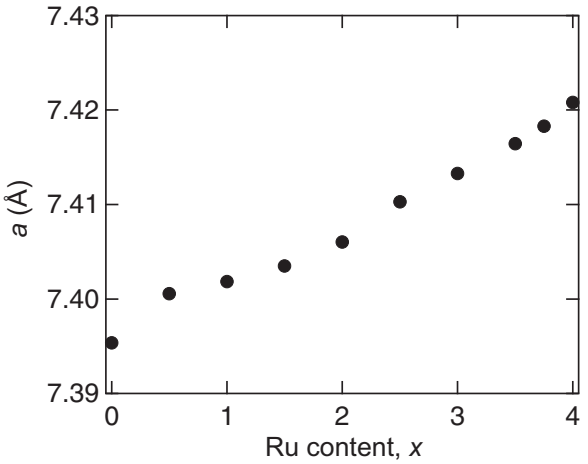

FIG. 4. Lattice constant of $CaCu_3Ti_{4-x}Ru_xO_{12}$ samples without chemical phase separation.

The susceptibility of each composition in the solid-solution system has a strong dependence on the temperature for smaller values of x, which is similar to Curie-Weiss behavior, or a weak dependence for larger values of x. The border between the strong and weak dependencies appears around $x = 1.5-2.5$, where the reciprocal susceptibility at 250–300 K becomes large. This classification is depicted more convincingly on a logarithmic plot [see Fig. 5(b)]. For $x = 1.5-2.5$, the reciprocal susceptibility on the logarithmic plot is convex upward unlike that for a smaller value of x, suggesting that the change from the strong to weak dependence is also caused by the temperature. Although the temperatures at the changes are difficult to determine because of the gradual changes, the changes roughly occur at the temperatures indicated by the arrows in Fig. 5(b). The temperatures at the changes appear to decrease with increasing x.

For low values of x, one may expect that the susceptibility obeys the Curie-Weiss law and that the deviation from the linearity of the reciprocal susceptibility is caused by a temperature-independent term. Thus, the reciprocal susceptibility between 50 and 320 K for $x \leqslant 3$ was fit using the function $\chi^{-1} = [C/(T-\Theta)+\chi_0]^{-1}$, where C, Θ, and χ_0 are the Curie constant, Weiss temperature, and a constant term, respectively. The parameters obtained are shown in Figs. 6(a) and 6(b). The strong temperature dependence represented by the Curie-Weiss term is rapidly suppressed with increasing x, while the weak dependence represented by the constant term increases. These features qualitatively agree with a previous report [8]. However, it should be noted that the Curie-Weiss behavior may not be applicable, even to the susceptibility for low values of x. The values of the parameters depended on the temperature range of the fitting, as shown in the Supplemental Material [18], which indicates that they are not very reliable and suggests that the Curie-Weiss behavior is invalid for the present system. The fitting-range dependence was significant for the fitting for $x \geqslant 1.5$, as shown in the Supplemental Material [18], supporting the change in the temperature dependence by the temperature. Moreover, for $x = 0$, the fitting parameters were unexpectedly dependent on the fitting range. As more data at low temperatures

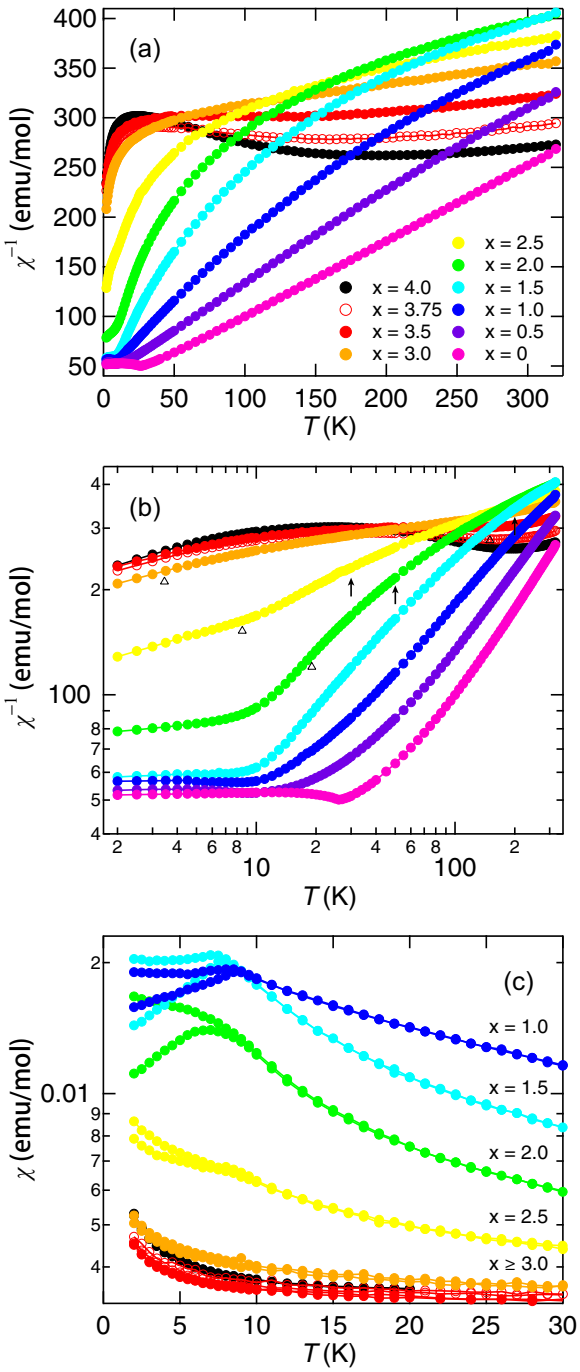

FIG. 5. Reciprocal magnetic susceptibility of $CaCu_3Ti_{4-x}Ru_xO_{12}$ for $x = 0$–4 (a) and (b) at 1 T and magnetic susceptibility (c) at 0.001 T. (b) The data appearing in (a) on a logarithmic scale. The arrows and triangles in (b) are explained in the text.

were included, the Curie constant and Weiss temperature increased and decreased, respectively. For example, the reciprocal susceptibility between 50 and 100 K, between 50 and 320 K, and between 200 and 320 K resulted in $C = 1.66$ (emu K)/mol and $\Theta = -48.0$ K, $C = 1.36$ (emu K)/mol and $\Theta = -35.0$ K, and $C = 1.32$ (emu K)/mol and $\Theta = -31.5$ K, respectively. One may attribute the unexpected dependence on the fitting range for $x = 0$ to the change in the electronic states discussed in a previous study [22]. The

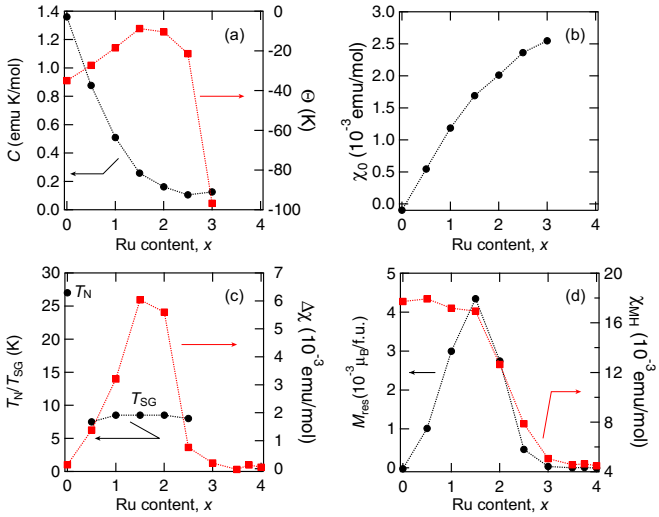

FIG. 6. (a) Curie constant C and Weiss temperature Θ. (b) Constant term χ_0. (c) The spin-glass-like transition temperature T_{SG} and the difference in the magnetic susceptibility $\Delta\chi$ at 2 K between the ZFC and FC data. (d) The slope and M intercept of the magnetization curve at 2 K.

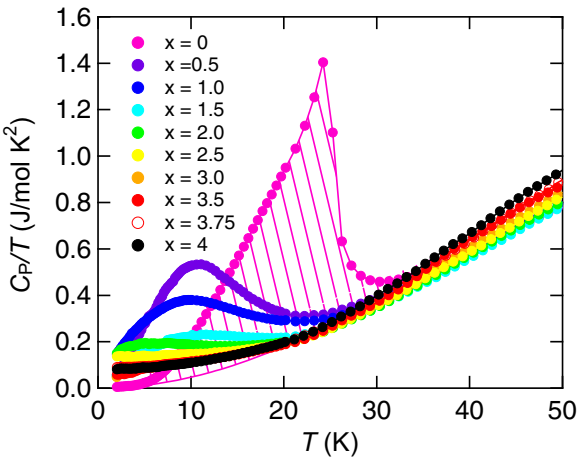

FIG. 7. Specific heat as a function of the temperature for $CaCu_3Ti_{4-x}Ru_xO_{12}$.

effective moment may be calculated from the Curie constants to be $p_{\rm eff} = 2.10$–1.88, which corresponds to the g value of $g = 2.43-2.17$. The g value is typical of that for Cu^{2+} ions [23–25] and agrees with that estimated by electron spin resonance (ESR) measurements [26]. Our experiments did not confirm the small moment reported previously [8].

For $x = 0.5-2.5$, the ZFC and FC magnetic susceptibilities at 0.001 T deviate from one another below $T_{SG} \sim 8$ K, as Fig. 5(c) shows. Spin-glass-like behavior has also been observed in a previous report [8]. The values of T_{SG} and the difference in the susceptibility $\Delta\chi$ at 2 K at 0.001 T are plotted in Fig. 6(c). The spin-glass-like transition temperatures are almost constant with x, as reported previously [8]. $\Delta\chi$ increases with increasing x up to $x = 1.5$ and then rapidly decreases to almost zero at $x = 3.0$. It should be noted that the ZFC susceptibility has a sharp peak at $x \leqslant 1.5$, whereas the peak of the ZFC susceptibility for $x = 2.0$ is blunt. The $x = 2.5$ sample displays no peak in its ZFC susceptibility but does show a gradual separation between the ZFC and FC susceptibilities below approximately 8 K. The origin of the blunt peak and the absence of the peak will be discussed later.

The x dependence of $\Delta\chi$ is confirmed by isothermal magnetization measurements at 2 K, which were performed from 1 to -0.1 T after the sample was cooled at 1 T from 320 K. The M intercept $M_{\rm res}$ and the slope χ_{MH} of the $M-H$ curves were estimated from the magnetization between 0.1 and -0.1 T by a linear function, as shown in Fig. 6(d). The values of $M_{\rm res}$ essentially show the same behavior as $\Delta\chi$. The small difference between them is probably due to the relatively large errors in the values of $\Delta\chi$; the magnetic field at each temperature-dependent measurement includes relatively large errors for the small field, and accurate ZFC conditions are difficult to achieve because of the residual magnetic field in the magnetometer. In contrast, χ_{MH} sharply changes from high values for $x \leqslant 1.5$ to low values for $x \geqslant 3.0$. The change in χ_{MH} occurs at the compositions of $2.0 \leqslant x \leqslant 2.5$, where the temperature dependence of the magnetic susceptibility changes as mentioned before.

The sharp changes in $\Delta\chi$ and $M_{\rm res}$ strongly suggest that the electronic states at 2 K discontinuously change with increasing x. Namely, a first-order phase transition occurs, which separates the electronic states with local magnetic moments and with itinerant electrons at approximately $x_t = 2-3$. It is supported by the sudden disappearance of T_{SG} at $x = 2.5$, although it occurs at approximately 8 K, and by the appearance of the mixed states, as shown later. The first-order transition is reasonable because the transition for eliminating local magnetic moments is usually first order, as mentioned in the Introduction.

For $2 \leqslant x \leqslant 3$, $M_{\rm res}$ and χ_{MH} linearly decrease with increasing x, suggesting the coexistence of two electronic phases in this range of x; their volume fractions change. From our preliminary ^{63,65}Cu NMR measurements for $x = 2.0$, we observed several resonance lines with different temperature dependencies of the spin-lattice relaxation rate, which may result from the mixed state. Mixed phases are observed in some systems showing first-order phase transitions. For example, κ-(BEDT-TTF)$_2$Cu[N(CN)$_2$]Br, which shows a first-order Mott transition by chemical substitution or the application of pressure, has a mixed state with two electronic phases beside the first-order phase-transition line [27]. For chemical substitution, the mixed state appears at a low temperature when about a quarter to half of the BEDT-TTF molecules are deuterated. This composition width is comparable to that of the present system. The mixed state has also been observed in some Mn oxides [28,29]. Mn oxides have both micrometer-sized clusters of antiferromagnetic charge-ordered states and ferromagnetic metallic states, which are stabilized by bond randomness caused by the mixed-valence state [30]. Thus, in the present compounds, the mixed state may be stabilized by the randomness at the B site. The first-order transition will be discussed in the next section.

C. Thermal properties

The specific heat of the samples is shown in Fig. 7. $CaCu_3Ti_4O_{12}$ shows a sharp peak at $T_N = 27$ K. The

magnitude of the peak agrees well with previous reports [31,32]. The entropy corresponding to the area shaded in Fig. 7 was estimated to be 11.3 J/(mol K), which is much smaller than the theoretical value of the spin entropy for $CaCu_3Ti_4O_{12}$, namely $3R\ln(2S+1) = 17.28$ J/(mol K) for $S = 1/2$ of Cu ions. The estimated value happens to be 2/3 of the theoretical one. The discrepancy in the spin entropy is likely caused by the weak first-order nature of the transition at T_N, as discussed in the next section.

For $x = 0.5$, 1.0, and 1.5, broad maxima appear at T_{SG}. The peaks share similar shapes, suggesting that their magnetic states are similar. The invariant peak position is consistent with the almost constant T_{SG}. The peak magnitude decreases with increasing x, which indicates that the number of the spins participating in the spin-glass-like state decreases with increasing x. This observation is reasonable because the magnetic state is probably related to the antiferromagnetic state for $x = 0$. The entropy was estimated to be 6.02, 4.97, and 2.72 J/(mol K) for $x = 0.5$, 1.0, and 1.5, respectively, assuming second-order transitions. It is interesting that, although the number of the spins decreases, the difference between the numbers of up and down spins increases with increasing x up to $x = 1.5$, as indicated by the x dependencies of M_{res} and $\Delta\chi$. This suggests that the substitution of Ti with Ru ions selectively eliminates the spins at certain magnetic sites.

The peak in the specific heat for $x = 2.0$ appears at a lower temperature than that for $x \leqslant 1.5$, and no peak is observed above 2 K for $x = 2.5$, although T_{SG} is almost constant at 8 K for $x \leqslant 2.5$. They appear to correspond to the blunt peak in the ZFC susceptibility for $x = 2.0$ and the absence of the peak for $x = 2.5$. Thus, the electronic phase separations at $x = 2.0$ and 2.5 are likely developing below T_{SG}, suggesting that the first-order phase transition line passes $x = 2.0$ and 2.5 around T_{SG}. The electrical resistivity supports this suggestion, as shown later.

The temperature dependencies of the specific heat for $x = 3.5$ and 3.75 behave similarly to that for $x = 4.0$, indicating the metallic nature of the compounds. The Sommerfeld constants for $x = 3.5$ and 3.75 were estimated from the specific heat between 8 and 15 K to be 89.2 and 89.5 mJ/(mol K^2), respectively. These values are slightly larger than 81.2 mJ/(mol K^2) for $x = 4.0$. However, it is not certain whether the values correspond to the carrier mass at 0 K. The $x = 3.5$ and 3.75 compounds may manifest phase separation below 8 K. Even if the phase separation does not occur at these compositions, the specific heat may increase below 2 K, just as in the case of $x = 4$ [14].

D. Electrical resistivity

Figure 8 shows the electrical resistivity, which decreases with increasing x at any temperature below 300 K. Insulating and metallic temperature dependencies are observed for $x \leqslant 1.0$ and $x \geqslant 2$, respectively. As shown in Figs. 8(b) and 8(c), the temperature dependencies for $x = 0.5$, 1.0, and 1.5 exhibit variable-range-hopping (VRH)-type behavior rather than Arrhenius-type behavior, which is likely caused by the randomness at the B site. Interestingly, the temperature dependence of the $x = 1.5$ sample has a minimum around $T_\rho = 150$ K. The minimum of the resistivity is also observed

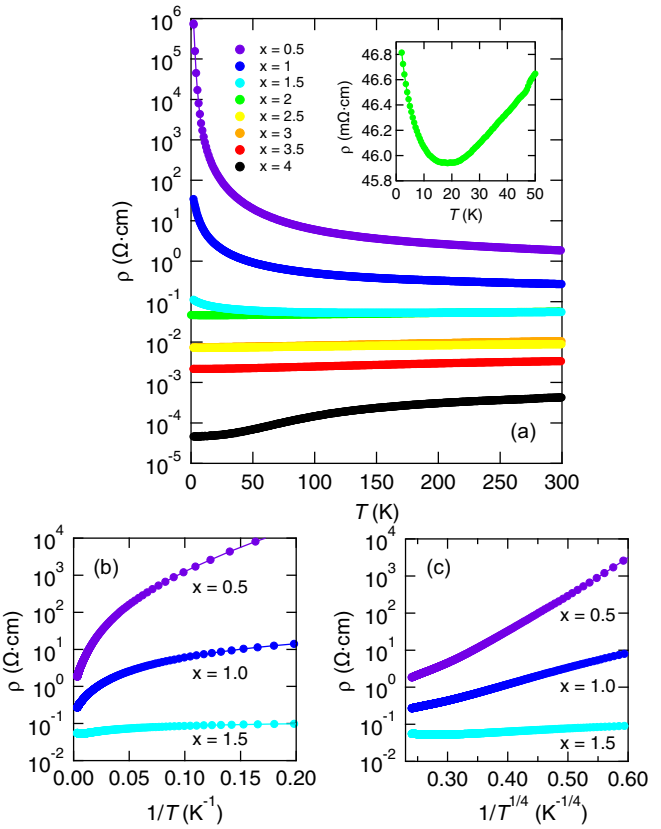

FIG. 8. Electrical resistivity of $CaCu_3Ti_{4-x}Ru_xO_{12}$. (b) and (c) Arrhenius and variable-range-hopping-type plots, respectively, for $x = 0.5$, 1.0, and 1.5. The inset of (a) shows the resistivity at low temperatures for $x = 2.0$.

for $x = 2.0$, 2.5, and 3.0 at $T_\rho = 19$, 8.5, and 3.5 K, respectively, as shown in the Supplemental Material [18]. T_ρ decreases with increasing x and separates the $x-T$ phase diagram for $x > 0$ into VRH and metallic regions at lower and higher values of x, respectively, as shown in Fig. 9. The border between the two regions roughly corresponds to the first-order phase-transition line because it is just beside the composition range for the mixed state, as in the case of an organic system [27].

The temperatures indicated by the arrows in Fig. 5(b), T_χ, are also plotted in Fig. 9. Although the errors in T_χ are difficult to estimate and presumably large, they obviously do not agree with T_ρ. The values of T_ρ are indicated by the triangles in Fig. 5(b), showing that they are much lower than T_χ. The difference between T_ρ and T_χ is likely caused by the difference in the characteristics of the properties. The magnetic susceptibility starts showing a strong temperature dependence when insulating domains with local magnetic moments appear with decreasing temperature. In contrast, the resistivity minimum appears when a portion of the insulating domains becomes so large that they disturb the percolation between the metallic domains and when the resistance of the insulating domains becomes significantly larger than the resistance of the metallic domains. In other words, insulating domains remain above T_ρ, as supported by the preliminary NMR data; the NMR resonance lines with different characteristics remain, at least

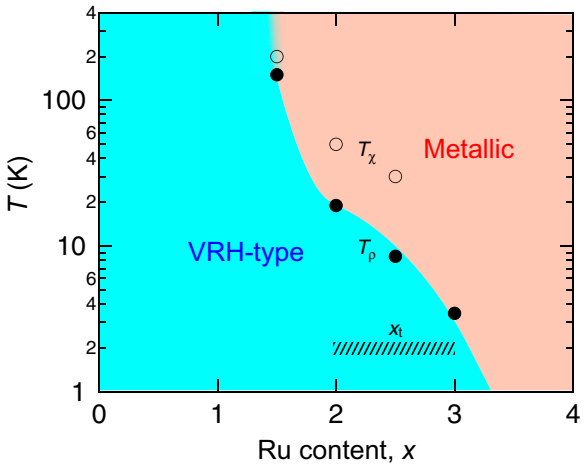

FIG. 9. Characteristic temperatures estimated from the resistivity (T_ρ) and magnetic susceptibility (T_χ) and characteristic compositions (x_t) estimated from $\Delta\chi$ and M_{res}, at which the magnetically mixed state is clearly recognized. The borderline between the VRH-type and metallic regions serves simply as a guide.

up to around T_χ. Phase separation over a wide temperature range has also been observed in an organic system [27].

IV. DISCUSSION

It is important to understand how the chemical composition x affects the electronic states of the compounds. According to electronic band structure calculations [11,33], the Cu $3d$ orbitals in $CaCu_3Ru_4O_{12}$ contribute to the density of states (DOS) at the Fermi level because of the hybridization between them and O $2p$ orbitals, whereas the Cu $3d$ orbitals in $CaCu_3Ti_4O_{12}$ do not make such a contribution despite the strong hybridization. The difference is caused by the ions at the B sites. In the former compound, Ru $4d$ orbitals are hybridized with O $2p$ orbitals, resulting in a significant contribution of O $2p$ orbitals to the DOS at the Fermi level. The energy level of the Cu $3d$ orbitals is shifted to the Fermi level together with the O $2p$ level. In short, CuO_4 molecularlike orbitals, which are formed by the strong hybridization between the Cu $3d$ and O $2p$ orbitals, are hybridized with Ru $4d$ orbitals to cause a significant partial DOS of Cu $3d$, O $2p$, and Ru $4d$ orbitals at the Fermi level. In contrast, in the Ti compound, the hybridization between CuO_4 molecularlike orbitals and Ti $3d$ orbitals is not significant and makes no contribution to the DOS at the Fermi level. Thus, the chemical composition x changes the mean hopping amplitude of the electrons/holes at the CuO_4 orbitals by controlling the average degree of hybridization between the CuO_4 orbitals and the d orbitals at the B sites.

The band structure of the Ru compound [11] can be explained more simply as follows. The upper and lower Hubbard bands of the CuO_4 molecularlike orbitals are bridged by Ru $4d$ orbitals, as in the case of a metal from a charge-transfer-type Mott insulator. In this sense, the present insulator-metal transition is a Mott transition. It is characteristic that the atomic orbitals of the cations connect the Hubbard bands; usually, the orbitals of anions, such as O $2p$ orbitals, bridge them.

One may expect that the substitution induces the pressure effect, as in the case of the organic compounds [34–36], because the substitution leads to the change in the lattice constant shown in Fig. 4. However, this idea does not apply to the present case because the lattice constant is larger in the metallic phase. A metallic state usually appears when a lattice is compressed because the overlap between the atomic orbitals in a compound is enhanced. It has been known that the electronic states of $CaCu_3Ru_4O_{12}$ and its related compounds are insensitive to changes in the lattice constant [9]. Our preliminary data for the solid-solution system of $Ca_{1-y}Sr_yCu_3Ru_4O_{12}$ also support this. In fact, the data showed that the magnetic susceptibility is almost independent of the Sr content, although the lattice constant increases up to 7.448 Å at $y = 1$, which is 0.3% larger than the $CaCu_3Ru_4O_{12}$ end member in Fig. 4.

The Ru ions in the present system play a more essential role in the occurrence of metallicity than simply expanding the lattice; as mentioned above, metallicity is induced by the hybridization between the CuO_4 and Ru orbitals. This implies that the electronic properties will be sensitive to the ions at the B sites and suggests that the B-site randomness is highly influential in the phase diagram. The mixed state beside the first-order phase-transition line is likely stabilized by the randomness, as in the case of Mn oxides [30].

The first-order phase-transition line will have end points, as in the case of an organic compound [27]. In this case, the end point at a higher temperature is the critical point where the transition is purely second order. Beyond this point, the insulating state with local magnetic moments continuously changes into the metallic state without local magnetic moments. Thus, the spin degree of freedom gradually disappears at a high temperature with increasing mean hopping amplitudes. More details about the elimination and emergence of the spin degree of freedom will be investigated by microscopic experiments, such as those examining NMR or muon spin rotation (μSR).

The opposite end point is likely located at $T = 0$ K as a critical point. The theory of Mott transitions [1] points out that a Mott transition at 0 K induced by a change in U/t (U: on-site Coulomb interaction and t: transfer integral) is continuous. The non-Fermi liquid behavior observed for $CaCu_3Ru_4O_{12}$ [14] may be related to the critical behavior of the Mott transition. We would like to point out that such critical behavior can appear even if the end point at $T = 0$ K is not a critical point; if the first-order nature is weak, critical fluctuations appear around the transition point without exhibiting a critical divergence. Thus, the expectation that the non-Fermi liquid behavior is related to the critical behavior of the metal-insulator transition discovered in this work is valid apart from the viewpoint of the Mott transition.

Finally, we speculate about the magnetic state of $CaCu_3Ti_4O_{12}$, although its elucidation lies beyond the scope of this paper. Despite the simplicity apparent at first sight, the magnetic state is not well understood; neutron scattering experiments have not succeeded in determining the magnetic structure [37], and some experiments for clarifying the magnetic state simply found unusual properties [26,31]. We found a 2/3 spin entropy, which is also unusual. In a previous report [32], the entropy was estimated to reach almost its full value around 60 K after an intermediate saturation around

40 K. The additional increase in the spin entropy from ∼40 to ∼60 K is caused by a decrease in the lattice contribution. However, such a decrease was not observed for any of our samples, although they shared the same crystal structure; the decrease should have been clearly observed, especially for the samples for $x \geqslant 3$, if it existed because the samples showed no magnetic transition. Furthermore, the large difference between T_N and 60 K is very strange because magnetic fluctuation over such a wide temperature range has not been observed; the Curie-Weiss behavior continues down to T_N. In addition, it should be noted that the absolute value of the Weiss temperature is much smaller than 60 K. The magnetic correlations usually develop only below $\sim|\Theta|$ because the Weiss temperature represents the magnetic correlations. One may assume that the entropy consumption below 60 K is consistent with the development of low-frequency magnetic Raman excitation, which has been reported to appear below 70 K [31]. The excitation has been attributed to short-range magnetic ordering. However, the excitation appears even at 305 K; therefore, it is unreasonable to regard the short-range ordering detected by Raman spectroscopy as the origin of the 2/3 entropy at T_N. The paper [31] points out the possibility that the short-range ordering is enhanced with light irradiation; hence, the magnon excitation observed by Raman spectroscopy bears no relation to the apparent entropy consumption just below 60 K. Therefore, our estimate of the spin entropy is reasonable, and the entropy is unusually small, as long as the antiferromagnetic transition is second order.

The 2/3 entropy suggests that the transition is, in fact, a first-order transition accompanied by a structural transition. The specific heat shows a sharp increase at T_N, which supports the first-order transition. Preliminary data acquired from μSR measurements indicate that the internal fields at muon sites, which correspond to the order parameter of the antiferromagnetic transition, decrease from 2 K to finite values at T_N and suddenly disappear just above T_N. Because the internal fields should continuously decrease to zero at T_N in the case of a second-order transition, the μSR results support the first-order transition.

Since the transition is first order, the antiferromagnetic transition is most likely accompanied with a structural modification. Nevertheless, the origin of the transition is magnetic because it occurs when antiferromagnetic fluctuations develop, as shown by the enhancement in the specific heat below 35 K. In most cases, structural transitions by antiferromagnetic ordering are induced by spin frustration to relax the frustration. In the present system, no geometrical frustration appears among the nearest-neighbor interactions, but spin frustration between the superexchange interactions and in-plane single-ion anisotropy in the CuO_4 squares can exist; in-plane collinear order is impossible because of the three types of CuO_4 squares with normals perpendicular to one another. Since collinear order is possible between only two of the three types of CuO_4 squares, the magnetic states are triply degenerate if collinear order is assumed. A structural transition may occur to lift this degeneracy. It is interesting that the ESR signals just below T_N are composed of paramagneticlike and antiferromagnetic components [26]. Their signal areas, which correspond to the numbers of spins participating in the signals, are comparable with one another. These observations clearly indicate that the Cu sites are not equivalent. The paramagneticlike component may originate from the spins at the CuO_4 squares left out of the collinear order. Spin frustration could be the origin of the selective elimination of the spins by the substitution of Ti with Ru ions.

V. SUMMARY

The solid-solution system of $CaCu_3Ti_{4-x}Ru_xO_{12}$ ($x = 0$–4) was successfully synthesized at 7.7 GPa at temperatures between 1300 and 1600 °C. The samples fabricated at lower temperatures were chemically phase separated for $x \leqslant 2.5$. The temperature below which the chemical phase separation occurs increases with decreasing x down to 0.5. The chemically uniform samples show an antiferromagnetic transition at $T_N = 27$ K for $x = 0$ and a spin-glass-like transition at $T_{SG} \simeq 8$ K for $0.5 \leqslant x \leqslant 2.5$. The magnetic susceptibility shows a strong dependence on the temperature for $x \leqslant 1.0$ and a weak dependence for $x \geqslant 3.0$ below 320 K. At intermediate values of x of $1.5 \leqslant x \leqslant 2.5$, the change from the strong to weak dependence occurs with decreasing temperature, and the temperature at which it occurs appears to decrease with increasing x. The residual magnetization at 2 K decreases with increasing x in the range of intermediate values of x. The slope of the magnetization curve at 2 K sharply changes from large values for $x \leqslant 1.5$ to small values for $x \geqslant 3.0$. The specific heat displays a sharp peak at T_N for $x = 0$ and a broad hump at T_{SG} for $x = 0.5$, 1.0, and 1.5. The shapes of the humps are similar, and their magnitudes decrease with increasing x. The $x = 2.0$ and 2.5 samples also show humps in their specific heat, but the humps appear at lower temperatures. The electronic resistivity shows VRH-type behavior for $x = 0.5$ and 1.5 below 300 K, whereas it shows metallic behavior for $x \geqslant 3.5$ below 300 K. For x in the range of $1.5 \leqslant x \leqslant 3.0$, the temperature dependence of the resistivity has a minimum. These properties indicate that the first-order insulator-metal transitions occur as functions of the temperature and composition. The first-order phase-transition line has a large negative slope, passing around $x = 1.5$ and $T = 150$ K and around $x = 3$ and $T = 3$ K. Electronic phase separation appears beside the transition line. The substitution of Ti with Ru ions enhances the hopping amplitude of the electrons/holes on the CuO_4 squares by bridging the lower and upper Hubbard bands of CuO_4 molecularlike orbitals. Thus, the insulator-metal transition is regarded as a Mott transition. The non-Fermi liquid behavior observed previously may be attributable to the critical behavior of the Mott transition. A structural transition and spin frustration are suggested for $CaCu_3Ti_4O_{12}$.

ACKNOWLEDGMENTS

Special thanks are given to Dr. T. Taniguchi for his support for high-pressure synthesis. We would like to thank Dr. M. Kohno, Dr. T. Kolodiazhnyi, Dr. M. Arai, and Dr. J. Inoue, National Institute for Materials Science (NIMS), for valuable discussions and Dr. Y. Matsushita for his support with the XRD measurements and analysis. This study is supported in part by Scientific Research C (JP16K05417 and JP17K05521) from the Japan Society for the Promotion of Science. T.-H.K. received support from the NIMS internship program.

[1] M. Imada, A. Fujimori, and Y. Tokura, Rev. Mod. Phys. **70**, 1039 (1998).
[2] L. Z. Liu, J. W. Allen, O. Gunnarsson, N. E. Christensen, and O. K. Andersen, Phys. Rev. B **45**, 8934 (1992).
[3] J. W. Allen and L. Z. Liu, Phys. Rev. B **46**, 5047 (1992).
[4] S. Doniach, Physica B+C **91**, 231 (1977).
[5] M. Subramanian, D. Li, N. Duan, B. Reisner, and A. Sleight, J. Solid State Chem. **151**, 323 (2000).
[6] A. Ramirez, M. Subramanian, M. Gardel, G. Blumberg, D. Li, T. Vogt, and S. Shapiro, Solid State Commun. **115**, 217 (2000).
[7] A. Collomb, D. Samaras, B. Bochu, and J. C. Joubert, Phys. Status Solidi A **41**, 459 (1977).
[8] W. Kobayashi, I. Terasaki, J.-i. Takeya, I. Tsukada, and Y. Ando, J. Phys. Soc. Jpn. **73**, 2373 (2004).
[9] A. Ramirez, G. Lawes, D. Li, and M. Subramanian, Solid State Commun. **131**, 251 (2004).
[10] H. Kato, T. Tsuruta, M. Matsumura, T. Nishioka, H. Sakai, Y. Tokunaga, S. Kambe, and R. E. Walstedt, J. Phys. Soc. Jpn. **78**, 054707 (2009).
[11] H. Xiang, X. Liu, E. Zhao, J. Meng, and Z. Wu, Phys. Rev. B **76**, 155103 (2007).
[12] S. Tanaka, H. Takatsu, S. Yonezawa, and Y. Maeno, Phys. Rev. B **80**, 035113 (2009).
[13] S. Tanaka, N. Shimazui, H. Takatsu, S. Yonezawa, and Y. Maeno, J. Phys. Soc. Jpn. **78**, 024706 (2009).
[14] A. Krimmel, A. Günther, W. Kraetschmer, H. Dekinger, N. Büttgen, A. Loidl, S. G. Ebbinghaus, E.-W. Scheidt, and W. Scherer, Phys. Rev. B **78**, 165126 (2008).
[15] T. Mitsuhashi, A. Watanabe, Y. Wada, Y. Onoda, and Y. Komatsu, Study on Ruthenium Titanates, NIRIM report 107 (National Institute for Research in Inorganic Materials, 1999).
[16] J. Málek, A. Watanabe, and T. Mitsuhashi, J. Therm. Anal. Calorim. **60**, 699 (2000).
[17] T. Mitsuhashi and A. Watanabe, J. Therm. Anal. Calorim. **60**, 683 (2000).
[18] See Supplemental Material at http://link.aps.org/supplemental/10.1103/PhysRevB.95.195141 for the details of sample characterization, Curie-Weiss fit, and electrical resistivity.
[19] T.-H. Kao, H. Sakurai, H. Kato, N. Tsujii, and H.-D. Yang, J. Phys. Soc. Jpn. **85**, 025001 (2016).
[20] V. J. Emery, S. A. Kivelson, and H. Q. Lin, Phys. Rev. Lett. **64**, 475 (1990).
[21] M. Ogata and H. Fukuyama, Rep. Prog. Phys. **71**, 036501 (2008).
[22] C. C. Homes, T. Vogt, S. M. Shapiro, S. Wakimoto, M. A. Subramanian, and A. P. Ramirez, Phys. Rev. B **67**, 092106 (2003).
[23] B. Bleaney and K. W. H. Stevens, Rep. Prog. Phys. **16**, 108 (1953).
[24] K. D. Bowers and J. Owen, Rep. Prog. Phys. **18**, 304 (1955).
[25] J. W. Orton, Rep. Prog. Phys. **22**, 204 (1959).
[26] M. C. Mozzati, C. B. Azzoni, D. Capsoni, M. Bini, and V. Massarotti, J. Phys. Condens. Matter **15**, 7365 (2003).
[27] T. Sasaki, N. Yoneyama, A. Suzuki, N. Kobayashi, Y. Ikemoto, and H. Kimura, J. Phys. Soc. Jpn. **74**, 2351 (2005).
[28] M. Uehara, S. Mori, C. H. Chen, and S. W. Cheong, Nature (London) **399**, 560 (1999).
[29] K. Lai, M. Nakamura, W. Kundhikanjana, M. Kawasaki, Y. Tokura, M. A. Kelly, and Z.-X. Shen, Science **329**, 190 (2010).
[30] A. Moreo, M. Mayr, A. Feiguin, S. Yunoki, and E. Dagotto, Phys. Rev. Lett. **84**, 5568 (2000).
[31] A. Koitzsch, G. Blumberg, A. Gozar, B. Dennis, A. P. Ramirez, S. Trebst, and S. Wakimoto, Phys. Rev. B **65**, 052406 (2002).
[32] I. Tsukada, R. Kammuri, T. Kida, S. Yoshii, T. Takeuchi, M. Hagiwara, M. Iwakawa, W. Kobayashi, and I. Terasaki, Phys. Rev. B **79**, 054430 (2009).
[33] L. He, J. B. Neaton, M. H. Cohen, D. Vanderbilt, and C. C. Homes, Phys. Rev. B **65**, 214112 (2002).
[34] S. Lefebvre, P. Wzietek, S. Brown, C. Bourbonnais, D. Jérome, C. Mézière, M. Fourmigué, and P. Batail, Phys. Rev. Lett. **85**, 5420 (2000).
[35] H. Ito, T. Ishiguro, M. Kubota, and G. Saito, J. Phys. Soc. Jpn. **65**, 2987 (1996).
[36] A. Kawamoto, H. Taniguchi, and K. Kanoda, J. Am. Chem. Soc. **120**, 10984 (1998).
[37] Y. Kim, S. Wakimoto, S. Shapiro, P. Gehring, and A. Ramirez, Solid State Commun. **121**, 625 (2002).